Eur. Phys. J. Appl. Phys. **44**, 11–19 (2008)
DOI: 10.1051/epjap:2008063

THE EUROPEAN PHYSICAL JOURNAL APPLIED PHYSICS

A combined FEG-SEM and TEM study of silicon nanodot assembly

P. Donnadieu[1,a], F. Roussel[2], V. Cocheteau[3], B. Caussat[3], P. Mur[4], and E. Scheid[5]

[1] SIMAP, INPGrenoble-CNRS-UJF, BP 75, 38402 Saint-Martin-d'Hères, France
[2] CMTC, INPGrenoble, Domaine Universitaire, BP 75, 38402 Saint-Martin-d'Hères, France
[3] LGC/ENSIACET/INPT, 5 rue Paulin Talabot, BP 1301, 31106 Toulouse Cedex, France
[4] CEA LETI -MINATEC, 17 avenue des Martyrs, 38054 Grenoble Cedex 09, France
[5] LAAS, avenue du Colonel Roche, 31077 Toulouse Cedex, France

Received: 9 July 2007 / Accepted: 22 February 2008
Published online: 30 April 2008 –

Abstract. Nanodots forming dense assembly on a substrate are difficult to characterize in terms of size, density, morphology and cristallinity. The present study shows how valuable information can be obtained by a combination of electron microscopy techniques. A silicon nanodots deposit has been studied by Scanning Electron Microscopy (SEM) and Transmission Electron Microscopy (TEM) to estimate essentially the dot size and density, quantities emphasized because of their high interest for application. High resolution SEM indicates a density of 1.6×10^{12} dots/cm^2 for a 5 nm to 10 nm dot size. TEM imaging using a phase retrieval treatment of a focus series gives a higher dot density (2×10^{12} dots/cm^2) for a 5 nm dot size. High Resolution Transmission Electron Microscopy (HRTEM) indicates that the dots are crystalline which is confirmed by electron diffraction. According to HRTEM and electron diffraction, the dot size is about 3 nm which is significantly smaller than the SEM and TEM results. These differences are not contradictory but attributed to the fact that each technique is probing a different phenomenon. A core-shell structure for the dot is proposed which reconcile all the results. All along the study, Fourier transforms have been widely used under many aspects.

PACS. 68.65.Hb Quantum dots – 68.37.Hk Scanning electron microscopy (SEM) – 68.37.Lp Transmission electron microscopy (TEM)

1 Introduction

During the last few years, silicon nanodots have attracted interest because of their unique physical properties. The quantum effects due to the nanodot size allow to develop new silicon based functional devices like resonant tunnel components, one dimensional transport devices, silicon nanocrystal memories and single electron transistors. Various methods have been considered for Si nanodot synthesis such as chemical vapor deposition, ion implantation, aerosol... However, floating gate memory applications need dot densities of about 10^{12} dots/cm^2 for 5 nm diameter dot [1]. To meet such requirements, Low Pressure Chemical Vapor Deposition (LPCVD) technique seems to be the most appropriate synthesis method [2].

Nanodots are deposited on monocrystalline silicon wafers covered with a few nanometer layer of thermally grown oxide. In the LPCVD process, the Si nanodots can be obtained from silane diluted in nitrogen, pure disilane or silane at temperatures between 673 K and 973 K and pressures between 0.2 and 10 Torr. To obtain nanoobjects, the deposition time has to be short (from few seconds to few minutes), hence the nanodot formation occurs during a transient regime. Besides the dot deposit is sensitive to many parameters such as the treatments used to modify the surface bonds. For instance, after a hydro fluoric acid treatment of the substrate, higher densities of nanodots can be obtained, namely over the 10^{12} nanodots/cm^2 range [3].

For device industrial production, the process must produce nanodots with controlled size, size distribution and density. For the LPCVD process, such control needs a large effort in modelling because the nanodots are formed in the transient regime [4]. Besides, numerous phenomena such as convective transport and diffusion occurring within the reactor and near the substrate; chemical reactions between gaseous species and with surface bonds have to be considered. Hence to be validated, the LPCVD process modelling has to be supported by high resolution characterization techniques. However, when high density nanoscale objects are deposited on a substrate, the separating distances are also nanometric which makes

[a] e-mail: patricia.donnadieu@simap.grenoble-inp.fr

characterization extremely difficult. Consequently the effort in modelling must be accompanied by a parallel effort in characterization to determine the dot size, densities, average distance, morphology and structure.

In spite of the development of new techniques and the improvement in the resolution of more classical ones, characterizing a dense assembly of nanodots remains a challenge. For instance, Atomic Force Microscopy (AFM) is not appropriate since its lateral resolution is limited by the convolution by the scanning probe shape which has a radius currently larger than 5 nm. Scanning Tunnelling Microscopy (STM) has the required resolution but cannot be employed routinely for studying series of samples. On the other hand, X-ray diffraction at grazing incidence can be carried out but because of the small quantity of matter a synchrotron source is necessary. Electron microscopy techniques appear as the most appropriate ones. On the one hand, Scanning Electron Microscopy (SEM) is now able to reach nanometric resolution owing to the Field Emission Gun (FEG) and the development of *in lense* secondary electron detector. It should be then possible to have the nanodot size and density of nanodot assembly using FEG-SEM. On the other hand, Transmission Electron Microscopy (TEM) can provide complementary information on the dot structure. In the present study, we are reporting on FEG-SEM observations completed by TEM investigations based on a recently developed phase retrieval imaging method and more classical approaches like high resolution transmission microscopy (HRTEM) and electron diffraction. Spectroscopic Ellipsometry (SE) which gives for a nanodot deposit the thickness of the equivalent layer has been also used as a test for the consistency of the electron microscopy measurements.

All the observations have been carried out on the same sample, i.e. a thermally oxidized (001) Silicon wafer on which nanodots have been deposited by LPCVD. More details on the related LPCVD modelling work as well as the synthesis conditions are given in [4,5]. Note that the aim of this article is not to report a systematic study of a series of nanodot samples but to illustrate how a relevant characterization can be obtained by combination of electron microscopy techniques. Besides, the complementarities of the techniques, the present work illustrates the large quantity of information that can be obtained under quite routine laboratory conditions.

2 FEG-SEM characterization of nanodot assembly

2.1 FEG-SEM imaging

A Zeiss Ultra 55 FEG-SEM has been used to make plan view images of the nanodot assemblies. No particular sample preparation or cleaning was done before imaging. To reach a better resolution, in this microscope, images are formed with a specific secondary electron detector which is based on the following ideas. The low-energy secondary electrons generated at the impact point of the primary electron beam are intercepted by a weak electrical field at the sample surface. They are then accelerated to a high energy by the field of the electrostatic lens and focused on an annular In-lens detector located above the objective lens. This detector provides high resolution information and gives better results on nanodots than the standard Everhart-Thornley detector, the usual lateral secondary electrons detector in the specimen chamber. The theoretical instrument resolution is 1 nm for an electron beam accelerated at 15 keV.

To get a good contrast for nanodots deposited on a substrate, a low accelerating voltage is chosen to reduce the volume of electron interactions. Typically at 15 keV the electron interaction volume is larger than 1 μm^3, i.e. several orders of magnitude larger to the dot size. Still, because of the thin insulating silica layer between the wafer and the dot deposit, the interaction volume must be large enough to insure electron conductivity. At low voltages, the images appear blurred because of charge accumulation. The image (Fig. 1a), obtained at 8 keV accelerating voltage, illustrates the best compromise in terms of dot contrast and charge effect. Unfortunately, a 8 keV accelerating voltage does not allow to benefit from the full instrument resolution, the equipment being optimize for the 15 keV operating conditions.

The FEG-SEM images obtained in the above conditions provide valuable information on the deposit quality. The dots are clearly nanometric and forming a dense assembly but the images suffers from a poor contrast. In particular, the dot signal is small in comparison with the long range intensity fluctuations (50 nm and above). Since the nanodots are on a much lower scale than the intensity fluctuation one, the image quality can be improved by a Fourier filtering. A convenient solution is to use a pass band filter to cut the non significant information at high and low frequency.

The filtering has been carried out using FFT transform and a mask to remove fluctuations below and above the range of the nanodot relevant information. The filtering has been applied to the FFT (Fig. 1b) of the image in Figure 1a. As shown by Figure 1c, the filtering is done in Fourier space by applying an annular mask with Gaussian edges, the mask radi are chosen to cut information above 20 nm and below 2 nm. Inverse FFT applied to the masked FFT gives the filtered image shown in Figure 1d.

The improvement obtained by filtering is significant. It can be easily checked that no information on the dot is missing but details which were rather guessed in Figure 1a are now seen with a better contrast. However the contrast is not good enough to allow for an particle counting using image analysis software. A semi manual method has been used to detectec and count the particles, it gives a density of 1.6×10^{12} /cm^2. Regarding the dot size, there are numerous small dots of about 5 nm as well as larger ones (about 10 nm). For these larger dots, the contrast is frequently inhomogeneous as if they were aggregates of smaller dots. As the large dots represent more than 10% of the assembly, it is clear that a resolution adapted

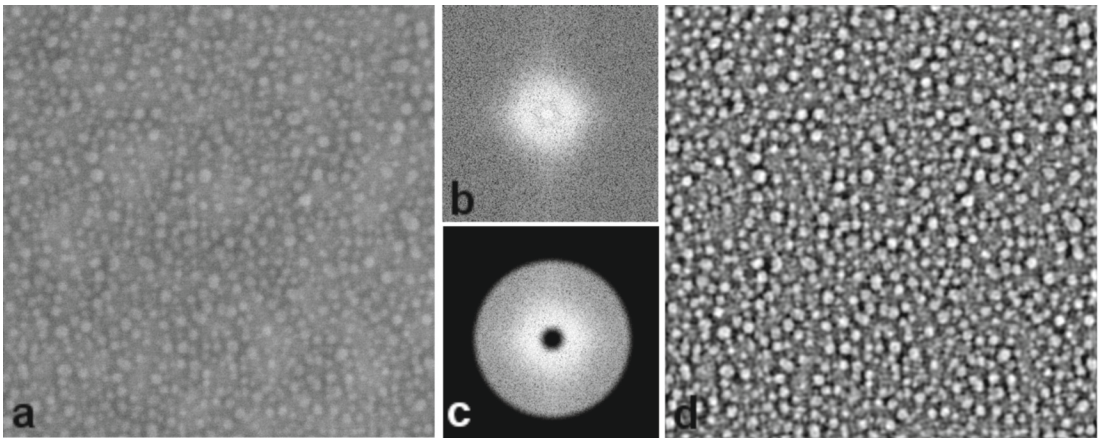

Fig. 1. (a) FEG-SEM image of the nanodot deposit obtained with a 8 keV accelerated voltage. (b) FFT of Figure (a), (d) image obtained by filtering according to the pass band filter shown in (c).

to the separation distance is necessary for a quantitative analysis.

Indeed, for nano-object which are close to the instrument resolution, it is not easy to know whether the resolution is sufficient or not because of the degradation of resolution inherent to the sample features (charging effects, object morphology, ...). At that stage, it is particularly interesting to use information given by a different technique (here Spectroscopic Ellipsometry (SE)), to test the consistency of the FEG-SEM results and to estimate how far the results can be from reality.

2.2 Spectrometric Ellipsometry measurements as a test for FEG-SEM results

Ellipsometry is a non contact and non destructive optical method currently used to measure the thicknesses of thin films [6]. It consists in measuring the polarization changes of a wave reflected by the surface of interest. Depending on the polarization, after reflexion the electric field components show specific attenuation and phase shift. In Spectroscopic Ellipsometry (SE), the wave length of the incident wave is usually scanned over the range 250 nm to 750 nm. The results (namely amplitude wave ratio and phase shift) are displayed then as spectra. By comparison of simulated spectra to the experimental ones, the film thickness as well as the refractive and extinction indices can be determined.

For discontinuous layers such as silicon nanodot assemblies, the SE results are interpreted using the Bruggeman effective medium approximation which describes the system as a multi-constituent stack of vacuum, amorphous and crystalline silicon [6]. The thickness of the equivalent continuous layer and the fractions of amorphous and crystalline silicon are determined using a numerical iterative solution starting from a set of initialization parameters. This method is routinely used as a characterization technique of thin films (see for instance [7]). It is worth noting that this indirect method allows also to determine the dot structure (crystalline or amorphous). Regarding nanodot deposit, the equivalent thickness layer can be used to estimate an average dot size knowing the dot density and assuming a particular dot shape. For a hemispherical shape of the nanodots, the mean diameter D is then given by the relation

$$D = 2\left(\frac{3e_{Si}}{2\pi d}\right)^{1/3} \quad (1)$$

where e_{Si} is the thickness of the equivalent silicon layer and d the density measured, for instance, with the FEG-SEM images.

For the sample previously studied by FEG-SEM, SE measurements indicates that the dots are crystalline and that the equivalent thickness is $e_{Si} = 1.38$ nm. Since the dot density according to FEG-SEM is $d = 1.6 \times 10^{12}$ dots/cm^2, it gives a mean diameter $D = 7$ nm. This value seems quite overestimate with respect to the FEG-SEM images showing a large number of dots in the 5 nm range. This can be interpreted by an underestimation of dot density because a lack of resolution of FEG-SEM as was already suggested by the large dot with irregular contrast. The SE measurements confirm then that it is necessary to use characterization techniques of higher resolution. TEM observations have been then carried out in order to measure more precisely the density and dot size and try to investigate in more details the dot shape and structure.

3 Phase retrieval TEM images

The easiest way to study by TEM nanodots deposited on a substrate is to prepare a plan view sample. The sample is first mechanically polished on the substrate side to a thickness of about 50 μm and further thinned to electron transparency by chemical etching or by ion polishing. The final polishing does not remove all the substrate, the area suitable for TEM observations are then made of a remaining thin slice of substrate covered by the nanodot deposit.

Nanodots can be imaged in TEM owing several types of contrast. First if the dots are crystalline, Dark Field

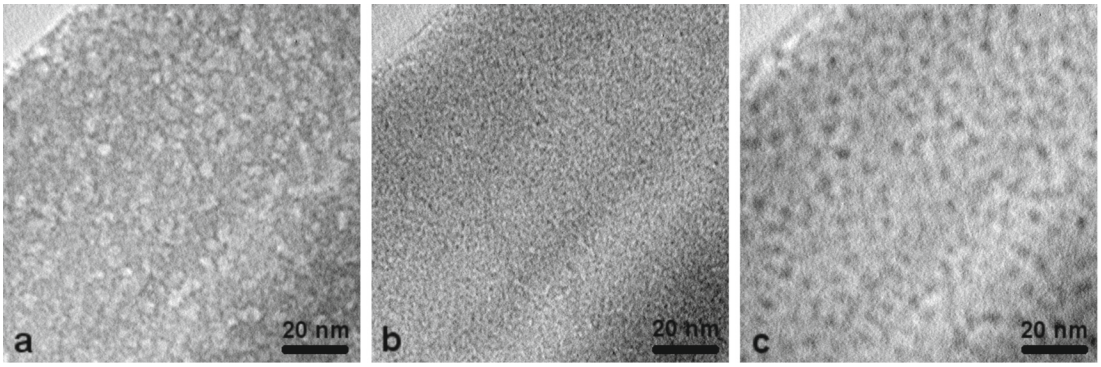

Fig. 2. TEM plan view images of a same area taken at different defocus Δ (a) $\Delta - 625$ nm, (b) $\Delta = 0$, (c) $\Delta + 625$ nm. Note the change on contrast and detail size when the defocus changes.

(DF) images can be carried out but as this image formation proceeds with a selection of intensity by the objective aperture only a part of the dot assembly is imaged. Hence to obtain the actual density from the one given by DF images, a correction factor depending mainly on the objective aperture and particle size should be determined first. Hence without a specific study to establish the correction factor, the DF images give essentially the dot size but not the dot density. Recently, Puglisi et al. [8] have successfully imaged nanodots by Energy Filtered Transmission Electron Microscopy (EFTEM) owing to a specific electron energy loss. Using a plasmon mode characteristic of collective electron excitations in Silicon, EFTEM images are appropriate for measuring the dot size and density [8]. On the other hand, according to TEM image formation theory [9], nanodots constitute typical case of phase contrast object, more precisely weak phase object. Hence it is possible to use the phase contrast for imaging the nanodots. The advantage of the phase contrast images is that they can be carried out on standard TEM equipment while for instance EFTEM imaging requires an electron energy loss filter. The other characteristic of the phase contrast is to be sensitive to the defocus of the objective lens. This effect is interesting in terms of contrast enhancement but the inconvenient is that the white or black dots on the image cannot be directly interpreted as nanodots. However a series of images taken at different defocus (i.e. a focus series) followed by a specific numerical treatment allows to retrieve a phase image and then measure the dot size and density. Such kind of approach which is detailed in [10] (and only briefly recalled below) is called a phase retrieval method. It is used here to complement the FEG-SEM study since the resolution for a $\pm$500 nm focus series is $\sim$1 nm [10].

3.1 The phase retrieval method

The phase retrieval method used here being detailed in [10], only the final step allowing to retrieve the phase from a focus series is given here. A series of 3 images taken at 3 defocus, namely $I(-\Delta z), I_0, I(\Delta z)$ respectively taken at $-\Delta z$, 0, Δz allows to retrieve the phase shift $\Phi(r)$ (or its Fourier transform) from the difference between images ΔI according to the relation:

$$\hat{\Phi}(q) = \frac{1}{I_0}\frac{1}{2\pi\lambda q^2}\frac{\Delta\hat{I}(q)}{\Delta z}$$

where the sign $\hat{}$ refers to the Fourier Transform.

Using the above equation, the phase image is derived by a FFT processing carried out on the series of images taken at Δz, 0 and $-\Delta z$ defocus. A small mask with Gaussian edge is used to avoid divergence due to the singularity in $q = 0$. Finally, from a series of 3 images, a phase image is obtained which contrast is directly proportional to the local sample thickness. As illustrated below, the phase image can give the dot density, size and mutual distance. It should also be possible to measure the dot height as pointed out in the discussion (Sect. 5).

3.2 Dot size, density and mutual distances

Figure 2 shows the focus series obtained for the nanodot assembly, previously studied by FEG-SEM. This series has been recorded on a CCD camera fitted on a Jeol 3010 microscope operating at 300 keV ($\lambda = 0.00197$ nm).

From this experimental series, the phase image can be computed according to equation (4) by writing the appropriate routine in image analysis software like Digital Micrograph or ImageJ [11]. Figure 3a shows the phase image retrieved from the focus series. The phase image is given as a plan view (Fig. 3a) as well as a 3D representation (Fig. 3b) in order to emphasize on the meaning of the contrast, i.e. the thickness fluctuations due to the dot assembly. The dot density estimated from the phase image is 2×10^{12} dots/cm^2. This density is obtained by manual counting since, in the present working conditions, the contrast was not high enough to allow for an automatic image analysis. The dot size estimated from a series of measurements is 5.2 nm $\pm$ 1.5 nm. It is worth noting that opposite to FEG–SEM images, we do not observe dots larger than 10 nm.

On the phase image in Figure 3a the dot distribution seems quite homogeneous. Since the organization of nanodots is a major point with respect to applications, a Fourier transform of the image has been done to test

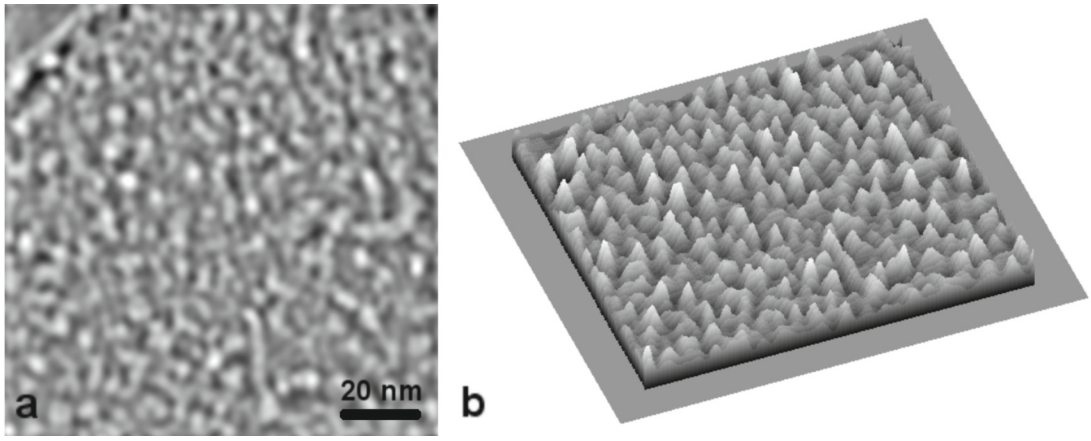

Fig. 3. Phase image corresponding to the area imaged in the focus series in Figure 2. (a) Plan view, (b) 3D representation of figure (a).

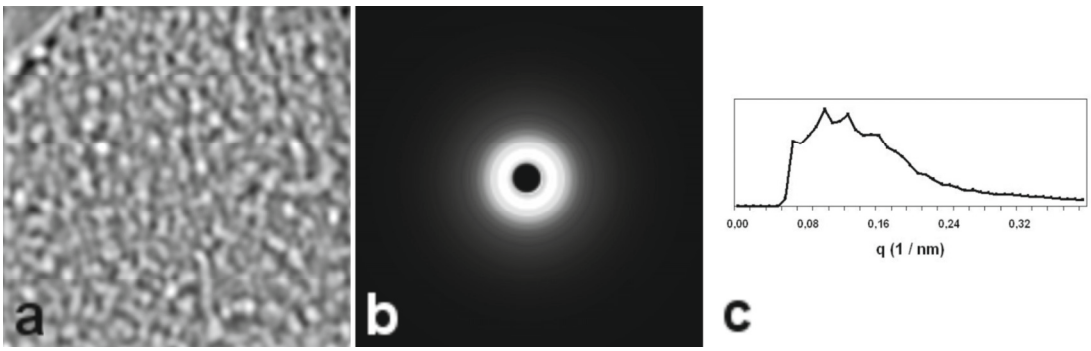

Fig. 4. (a) Phase image of the nanodot assembly. (b) FFT of the phase image after applying a rotational average. The intensity maximum in $q = 0$ is cut by a mask of small radius (0.04 nm^{-1}). (c) Profile of intensity of the FFT after averaging. A maximum in the intensity profile is observed for $q_{max} = 0.13$ nm^{-1}.

whether there is a characteristic average distance between dots. The Fourier transform is obtained from the phase image by FFT algorithm followed by a rotational average to derive the intensity profile. A mask of small radius ($q = 0.04$ nm^{-1}) has been applied to remove the intensity maximum in $q = 0$, insignificant in terms of dot distances. Figures 4a–4c display the starting phase image, the FFT after rotational average and the intensity profile. This profile is characterized by a maximum which reveals a mean distance between dots. The position of the maximum is $q_{max} = 0.13$ nm^{-1} corresponding to a mean distance between dots $d = 7.7$ nm.

The SE results can again be used to test the validity of the TEM phase image results. For the density 2×10^{12} dots/cm^2, the dot diameter according to the SE thickness interpretation is $D = 6.4$ nm. This value is close but a little larger to the one measured on the phase image.

As for the FEG-SEM results, this underestimation can be also interpreted as a lack of resolution with the TEM phase retrieval method. Indeed the present working conditions were not the most appropriate (in particular an indirect illumination type CCD camera was used). A more sensitive direct CCD camera should help to reduce the noise on the final phase image and then improve the spatial resolution.

4 On the dot structure and morphology

The TEM phase images and the FEG-SEM ones give no indication on the nature of the dots (crystalline or amorphous). The HRTEM imaging mode and electron diffraction can then be used to clarify this point.

4.1 HRTEM imaging on nanodots

HRTEM is quite easy to carry out on a dense assembly of dots since some of them are always correctly oriented to give at least fringe image. As illustrated by Figure 5a, the nanodots can be recognized as domain formed of about 10 fringes, the distance between fringes is about 0.310 ± 0.005 nm which is consistent with the (111) plane spacing in Silicon (0.313 nm). For noisy HRTEM image, the now well known geometrical phase image method developed by Hytch et al. provides an efficient tool to measure the size of domain which can be difficult to identify with only the fringes [12]. The geometrical phase image (Fig. 5b) is derived by a Fourier processing applied to the HRTEM image (Fig. 5a) according to the method described in [12]. In Figure 5b, the area with constant grey level correspond to a crystalline domain defined by the selected g vector (here a (111) vector). According to

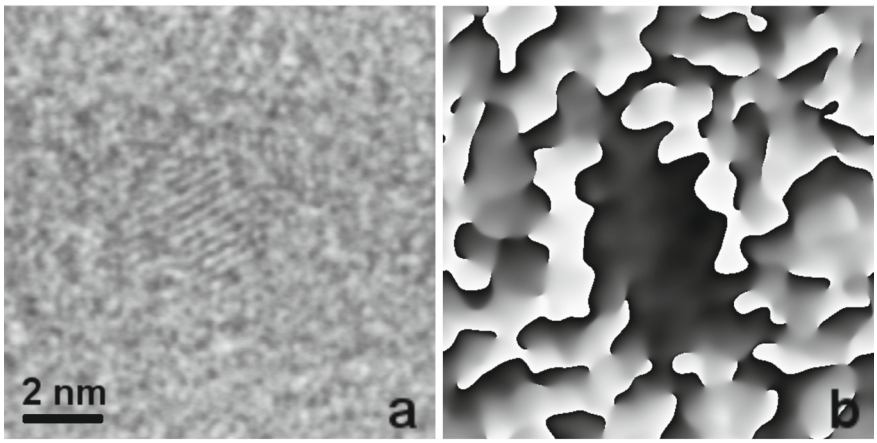

Fig. 5. (a) HRTEM image taken on the plan view sample. The fringes can be identified as crystalline nanodot, the fringe spacing is 0.31 which is consistent with the (111) spacing in Silicon. (b) Geometrical phase image for the selected g (111) vector corresponding to the fringes in 5a. The area with constant grey level allows to identify the crystalline domain.

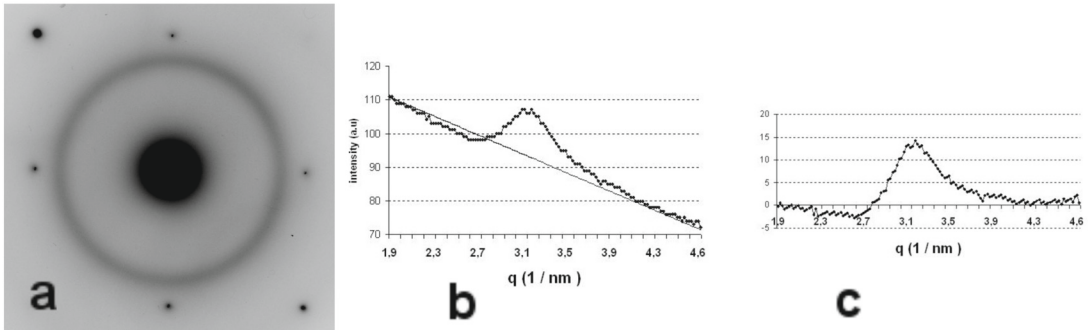

Fig. 6. (a) Electron diffraction pattern recorded on the nanodot deposit. The diffuse ring position is consistent with the (111) spacing in silicon. (b) Intensity profile of the diffuse ring after rotational average. The straight line estimates the background intensity. (c) Intensity profile of the ring after background subtraction, the ring width is $\Delta q = 0.43$ nm^{-1}.

the HRTEM image, the crystallite is rather small (about 3 nm). On the corresponding geometrical phase image which slightly emphasizes the size, the crystallite domain is also quite small (about 2 nm by 5 nm in Fig. 5b). Other HRTEM images have also given small domain size compared to the ones measured with the TEM phase retrieval method and the FEG-SEM images.

However HRTEM allows only the observation of a limited number of dots, electron diffraction is worth trying since it provides more global information on crystallinity as well as the domain size.

4.2 Electron diffraction on the nanodot deposit

Figure 6a gives the electron diffraction pattern obtained on the plan view sample previously studied by TEM. It is characterized by two types of features: a spot pattern indexable as the Silicon ⟨001⟩ zone axis, a diffuse ring centred on a position close to 0.32 nm in agreement with the (111) spacing in Silicon (0.313 nm). Diffuse rings are generated by an homogeneous distribution of small objects, here the nanodots. The positions of the diffuse ring indicate that the dots are crystalline. Besides a weak second ring consistent with on the (220) Silicon distance was also observed for long exposure time.

The diffuse rings are characterized by a significant width which can be measured on electron diffraction like Figure 6a. As the diffuse ring intensity is quite weak, a rotational average has been applied to obtain a less noisy profile. Figure 6b shows the intensity profile of the diffuse rings of Figure 6a. Figure 6c displays the same profile after background subtraction. The width at half maximum intensity is equal to $\Delta q = 0.43$ nm^{-1} which corresponds to a length $\ell = 2.3$ nm.

Crystallite finite size as well as defects and strain are responsible for widening and/or changes in the intensity profiles of the diffraction lines. For nanocrystals, the size effect is expected to be the major reason for the diffraction line width because the effect is inversely proportional to the crystallite size. Therefore in the following analysis only the size and shape of the dots are considered, the strain and defects are neglected.

According to diffraction theory, the widening due to size effect results from the convolution of each reciprocal point by the Fourier transform of the function describing the crystallite shape in direct space. Hence a crystallite with a given size and shape is characterized by a shape factor $F(q)$ (i.e. the Fourier transform of the shape function $f(x)$) [13]. However as far as intensity rather than amplitude are measured, the quantity of interest is the

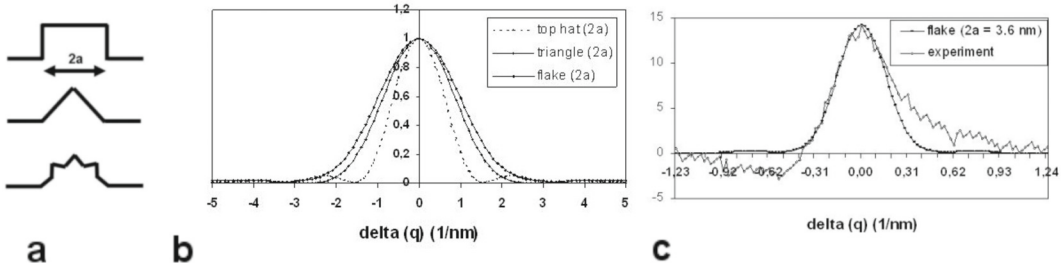

Fig. 7. (a) 2 dimensional model shapes of the nanodots: a top hat function, a triangle and a simplified snow flake; all shapes are taken with a same basis width 2a. (b) Square module of the shape factor calculated for different shape function. The width at mid peak height is: $\pi\Delta qa = 1.4$ (top hat function), $\pi\Delta qa = 2$ (triangle), $\pi\Delta qa = 2.4$ (flake). (c) Comparison between the experimental intensity profile of the diffuse ring and a calculated shape factor corresponding to the simplified snow flake shape with basis $2a = 3.6$ nm.

square module of the shape factor

$$|F(q)|^2 = \left| \int f(x) e^{-2i\pi q.x} dx \right|^2 .$$

To analyse in more details the relation between the dot size and the ring width, the shape factor has been calculated for several 2D hypothetical shapes (Fig. 7a), namely a top hat function (width 2a), a triangle (basis 2a), a simplified snow flake (basis 2a).

Figure 7b shows the intensity profile expected from the shape factor calculated for each of the model shapes. For simplifying, the abscissa axis is πqa where q is the reciprocal vector and a the size in direct space. Using the calculated intensity profile, for each shape the relation between characteristic size in direct space and width (Δq) in reciprocal space can be derived. It comes out: $\pi\Delta qa = 1.4$ for the top hat function (width 2a), $\pi\Delta qa = 2$ for the triangle (basis 2a), $\pi\Delta qa = 2.4$ for the simplified snow flake (basis 2a). Hence for a same Δq width, the corresponding size in direct space is somewhat smaller for a top hat function or triangle shape compared to a snow flake one. If we assume this shape for the dots, the dot size is $L = 2a = 3.6$ nm. Figure 7c illustrates the agreement which can be obtained between the experimental ring width and a snow flake shape factor with $L = 2a = 3.6$ nm.

However, this size which is in good agreement with the HRTEM observations is significantly smaller from the FEG-SEM and TEM phase images results. The difference is indeed about a factor of 2: 3–3.6 nm by HRTEM and electron diffraction against 5–7 nm by TEM and SEM. One can wonder whether more complex shapes could give a better agreement, i.e. provide an interpretation for the line width consistent with a larger dot size. Actually it is convenient to express the square module of the shape factor slightly differently than above.

$$\begin{aligned} |F(q)|^2 &= \left| \int f(x) e^{-2i\pi q.x} dx \right|^2 \\ &= \iint f(x) f(x') e^{2i\pi q.(x'-x)} dx dx' . \end{aligned}$$

This rewriting points out that the shape factor is related to the Fourier transform of the autocorrelation function of the dot shape in direct space. It means that even if the shape function was made more complex, for instance by adding more facets to the flake, large changes cannot be expected since the autocorrelation function will not be strongly affected by changes in the details. Indeed, this is already illustrated by the small variation between the width for a triangle compared to the simplified snow flake one. Consequently, a more complex flake could be expected to give a similar result and then cannot explained size differing by a factor of 2.

To discuss the sizes given by different techniques, it should first considered which aspects each technique is probing. For instance, in diffraction the size given by the line width is related to the one of the diffracting domain, i.e. the size of the domain in which diffracted waves are coherent enough to interfere. Such domain can be depicted as a "good" crystal one without to much strain and defects. In HRTEM, the dot size is given by the area in which lattice fringes can be imaged, this is also possible in a domain having a quite well defined crystalline structure. On the other hand, the TEM phase retrieval method sees the nanodots through the projected potential and is therefore less sensitive to the disorder or distortion within the dots. Regarding FEG-SEM images, since the secondary electron mode is essentially probing the topography, they are not sensitive to the dot structure. There is then an interpretation which can reconcile all the results: the dots are formed by a crystalline core of size $L \sim 3$–3.6 nm and a thin shell showing imperfect crystallinity. The nanodots will show then a larger size ($\sim$5 nm) or a smaller one ($\sim$3 nm) depending on the investigation technique.

5 Discussion

Using all the information that can be obtained from different electron microscopy techniques, we have been able to measure the density, the dot size and average mutual distance as well as giving information on the dot structure. In particular, from the comparison of techniques, we can propose a model for the dot consisting in a crystalline core and a shell of less defined structure. The external shell could be made of disordered Silicon but also formed by a thin oxidization layer. Evidence of such layer has been given by

XPS experiment on oxidized Silicon nanodots [14]. Further spectroscopy experiments (XPS of course and may be EELS) would be of interest to test this interpretation on Si nanocrystals with or without oxidation treatment. This points out again how important is the combination of techniques to achieve to a full characterization of nanoobjects. On the other hand, size or other structural details revealed by different characterisation techniques are usually related to specific physical properties. For instance, the size of crystalline domain should be relevant for quantum confinement effect while surface structure is expected to have a connection with screening [15].

Of course, some quantity remained to characterize like the strain within the dots. This information is present in the position and the intensity profile of the diffraction lines. This could be studied by X-ray techniques, for instance like GID (Grazing Incidence Diffraction). Still some preliminary experiments done on a synchrotron source have not allowed to derive information because of the weak intensity of the high indices lines. In that case, it should be interesting to consider what can be obtained electron diffraction. Of course recording the intensity of series of high indices lines required appropriate CCD cameras or imaging plates.

Strains within the dots contribute also to enlarge the diffuse ring. In that case the experimental ring width corresponds to the addition of shape and strain effect and then cannot be related simply to a size. The effect of strain and shape can be separated if rings corresponding several (hkl) lines can be measured. Finally, defects can also generate a broadening and particular asymmetry of the diffraction line. If several diffraction lines can be measured, it is possible in principle–but certainly difficult in practice–to separate the effect of size, strains and defects.

Improvement of the present electron microscopy results should be achieved in the near future. For instance, plasma cleaning of the sample before FEG-SEM imaging is now becoming routinely available. This sample preparation reduces the contamination layer which allows a lower scanning speed and then better signal/noise ratio at high magnification. Regarding the TEM phase retrieval method, numerous improvements can be done using. For instance, a more sensitive CCD camera will allow reducing the defocus and further having a better resolution. On the other hand, there is quantitative information in the phase value given by the phase retrieval processing. Indeed, opposed to the TEM starting images, the contrast in the phase image is related to the thickness fluctuations. For an homogeneous system, in each (x, y) point, the phase image intensity gives the thickness according to equation (3). For Silicon dots deposited on a substrate, the thickness fluctuation t is related to the phase fluctuation $\Delta\Phi$ by:

$$t = \frac{\lambda E \Delta\Phi}{\pi V} \tag{2}$$

where V is the inner potential. Hence, if this inner potential is known, the phase fluctuation can measure the dot height. A first approximation of the inner potential can be made from the structure factor data. However, it would be better to have more realistic potential. The numerous holography studies going on nowadays should provide reliable inner potential for Silicon. On the other hand, the development of atomistic calculations should also give values for the inner potential. This knowledge is necessary to derive more quantitative information from phase retrieval.

The major points illustrated by the present work is that, when different results are obtained by different techniques, there is not necessarily contradiction since each method is frequently based on a particular interaction with the sample. Hence, each technique is measuring a particular aspect. It is then important to gather all the information and try to propose a description which synthesizes all the results.

Finally it should be insisted that a lot of information is to expect from the experiments that can be carried out at the synchrotron owing to the X-ray spectroscopy (XPS) or the X-ray diffraction under grazing incidence. However these techniques test the whole assembly of particles. So they will always be fruitfully complemented by more local techniques like FEG-SEM and TEM. Besides, the strength point of the electron microscopy techniques is to make high resolution tools currently available in laboratory conditions.

6 Concluding remarks

The present work has been focused on the characterization of nanodots assembly that appears necessary with respect to the elaboration control required in view of applications. However such characterization remains quite a challenge in spite of the development of new techniques and the improvement in resolution of the electron microscopy ones. It is indeed difficult when dealing with nanoobjects to know whether the resolution is sufficient of not. The nanodots assembly studied here gives an illustration of the difficulties due to the small size of the object as well as small mutual distance in addition to possibly ill defined structure.

The study reported here can be considered as an exemplar investigation which proceeds, step by step, and by crossing different approaches. FEG-SEM and TEM techniques were particularly emphasized because they are the more accessible techniques and as shown here they succeed in giving much information like size, density, morphology... Of course it means pushing these methods to the maximum of their possibilities and making use of all the available analysis, especially the one based on Fourier analysis. Fourier based methods have been applied here as image treatment, as measurement tool for the dot mutual distance but also in the phase retrieval processing. For that specific aspect, nanodot assemblies constitute a system of choice for applying new method like the phase retrieval which is valid for phase contrast object.

In spite of the many interest of SEM and TEM imaging, one must stay open to non imaging techniques which can provide valuable test for the consistency of results. For instance, spectroscopic ellipsometry results have been used here to test the TEM and SEM results. But other

techniques like the X-ray diffraction or X-ray spectroscopy are clearly complementary to a SEM and TEM study.

The main conclusion of the present work is that there is no technique of choice. Each technique is testing a particular aspect of the system. Hence different results do not have to be opposed but rather to be reconciled. When dealing with very small scale, extreme care is required since the objects are frequently at the experimental resolution limit. Our strategy was to progress step by step using SEM and TEM imaging modes and getting from each technique the relevant information and trying to synthesize all the information in an appropriate structural model for the nanodots.

This work has been carried out, in the frame of CEA-LETI/CPMA collaboration, with PLATO Organization teams and tools.

References

1. S. Tiwari, F. Rana, K. Chan, H. Hanafi, W. Chan, D. Bucanan, Appl. Phys. Lett. **68**, 1377 (1996)
2. G. Nicotra, R.A. Puglisi, S. Lombardo, C. Spinella, M. Vulpio, G. Ammendola, M. Bileci, C. Gerardi, J. Appl. Phys. **95**, 2049 (2004)
3. F. Mazen, T. Baron, G. Bremond, N. Buffet, N. Rochat, P. Mur, M.N. Semeria, J. Electrochem. Soc. **150**, 203 (2003)
4. V. Cocheteau, B. Caussat, P. Mur, E. Scheid, P. Donnadieu, T. Billon, Electrochem. Soc. Proc. **9**, 523 (2005)
5. V. Cocheteau, Ph.D. thesis, INPT, France, 2005
6. M. Fried, T. Lohner, P. Petrik, in *Handbook of Surfaces and Interfaces of Materials* (Publisher, Academic Press, San Diego, CA, 2001), Vol. 4, pp. 335–367
7. M. Losurdoa, F. Rocab, R. De Rosab, P. Capezzutoa, G. Brunoa, Thin Solid Films **383**, 69 (2001)
8. R.A. Puglisi, S. Lombardo, G. Ammendola, G. Nicotra, C. Gerardi, Mat. Sci. Eng. C: Biomimet. Supramol. Syst. C **23**, 1047 (2003)
9. L. Reimer, *Transmission Electron Microscopy, Physics of Image Formation and Microanalysis*, 3rd edn. (Springer, Berlin, 1993)
10. P. Donnadieu, M. Verdier, G. Berthome, P. Mur, Ultramicroscopy **100**, 79 (2004)
11. Digital Micrograph (Gatan Inc. Pleasanton, CA, USA), ImageJ (free software `http://rsb.info.nih.gov/ij/`)
12. M.J. Hytch, E. Snoeck, R. Kilaas, Ultramicroscopy **74**, 131 (1998)
13. P. Hirsh, A. Howie, R.B. Nicholson, T.W. Pashley, M.J. Whelan, *Electron Microscopy of Thin Crystals*, 2nd edn. (Butterworths, London, 1965)
14. O. Renault, R. Marlier, M. Gely, B. De Salvo, T. Baron, M. Hansson, N.T. Barrett, Appl. Phys. Lett. **87**, 163119 (2005)
15. G. Allan, C. Delerue, Phys. Rev. B: Cond. Matt. Mat. Phys. **75**, 195311/1 (2007)